# UV-C Light Intervention as a Barrier against Airborne Transmission of SARS-CoV-2

**Izabela Ragan [1,*], Jessie Perez [2], Lindsay Hartson [3], Wilson Davenport [2] and Branden Doyle [2]**

[1] Colorado State University; Department of Biomedical Science, izabela.ragan@colostate.edu
[2] Violett Inc; Gig Harbor, WA jessie@violett.com, wilson@violett.com, branden@violett.com
[3] Colorado State University; Department of Microbiology, Immunology, & Pathology, lindsay.hartson@colostate.edu
[*] Correspondence: izabela.ragan@colostate.edu; Colorado State University, Infectious Disease Research Center, 3185 Rampart Rd, Fort Collins, CO, USA 80521; Tel.: +1-719-322-3331

**Abstract: Background:** SARS-CoV-2 continues to impact human health globally, with airborne transmission being a significant mode for transmission. In addition to tools like vaccination and testing, countermeasures that reduce viral spread in indoor settings are critical. This study aims to assess the efficacy of UV-C light, utilizing the Violett sterilization device, as a countermeasure against airborne transmission of SARS-CoV-2 in the highly susceptible Golden Syrian hamster model. **Methods:** Two cohorts of naïve hamsters were subjected to airborne transmission from experimentally infected hamsters; one cohort was exposed to air treated with UV-C sterilization, while the other cohort was exposed to untreated air. **Results:** Treatment of air with UV-C light prevented the airborne transmission of SARS-CoV-2 from experimentally exposed hamster to naïve hamsters. Notably, this protection was sustained over a muti-day exposure period during peak viral shedding from hamsters. **Conclusion:** These findings demonstrate the efficacy of the UV-C light to mitigate airborne SARS-CoV-2 transmission. As variants to continue to emerge, UV-C light holds promise as a tool to reduce infections in diverse indoor settings, ranging from healthcare facilities to households. This study reinforces the urgency of implementing innovative methods to reduce airborne disease transmission and safeguard public health against emerging biological threats.

**Keywords:** SARS-CoV-2; transmission; respiratory; viruses; healthcare; sterilization; air; hamster model; UV-C light; inactivation

## 1. Introduction

The SARS-CoV-2 global pandemic has killed over 6.9 million people and new variants are still emerging [1]. Over the course of the last three years it has become clear that the primary means of transmission from infected individuals is via respiratory, especially respiratory droplets [2]. In response, several strategies have been implemented to reduce airborne transmission and mitigate infection risk including stringent hygiene practices, social distancing, wearing masks, improving indoor ventilation, move gatherings to outdoor areas, altering indoor air humidity levels, and vaccination [3–7]. Within this context, a number of studies have highlighted the potential for UV-C light as a means to mitigate transmission of SARS-CoV-2.

Noteworthy is the finding that UV-C light doses of 34.9 to 52.5 mJ/cm² can inactivate SARS-CoV-2 on surfaces [10–12] and 21.4 mL/cm² dosing can inactivate SARS-CoV-2 in air [8] over brief exposure durations. The current study extends these findings by demonstrating the capacity of UV-C light to provide long term protection from airborne SARS-CoV-2 transmission over an extended multiday period. We employ a susceptible hamster model to demonstrate the long-term effectiveness of UV-C light as a means to inactivated SARS-CoV-2 in indoor settings and safeguard against airborne transmission.

## 2. Materials and Methods

### Violett Air Sterilization Device

The Violett sterilization device used a fan to draw air through a HEPA filter and into a UV-C light chamber. UV-C LEDs were used as they produce peak germicidal wavelengths of 265 nm with very tight emittance bands(+/- 5 nm) (Bulb S6060-DR250-W275-P100-V6.5). A control device was used to mimic standard air flow conditions by using a fan to pull air through the unit without HEPA filtration or UV-C LEDs. Both the experimental and control devices were connected to the animal housing with six feet of 3 inch diameter duct hose (Bio-R-Vac hose McMaster PN 56675K48).

### Animals

We used a total 27 male Golden Syrian hamsters (*Mesocricetus auratus*) at 7-9 weeks. All hamsters were held at Colorado State University in Association for Assessment and Accreditation of Laboratory Animal Care (AAALAC) International accredited animal facilities (Accreditation #000834). Animal testing and research received ethical approval by the Institutional Animal Care and Use Committee (IACUC). Hamsters were acquired from Charles River Laboratories (Wilmington, MA) and were maintained in a Biosafety Level-3 (BSL-3) animal facility at the Regional Biocontainment Lab at Colorado State University during the study.

### Study Design

Individually ventilated hamster cages were modified to create a closed system where air would enter the cage with infected hamsters and flow to peripheral cages with naive hamsters. The Violett device was connected to 3 inch diameter flexible tubing between the cages to allow treatment of air (Figure 1). The air exchange within the system was about 60 changes per hour. A total 27 hamsters were randomly divided into three groups of nine hamsters to complete three experimental replicates. Within each replicate three hamsters were randomly assigned to one of three groups: Infected, Violett-treated, or Control. Hamsters within the Infected group were infected intranasally with $1 \times 10^4$ pfu SARS-CoV-2 virus (USA-WA1/2020) under sedation and co-housed in the central cage for 24 hours. Prior to the addition of naïve hamsters, the sterilization devices were turned on for 15 minutes to ensure proper function. Next, with the devices continuously running, three naïve hamsters are introduced into each of the two peripheral cages (total of six hamsters). The device remained on for a total of 48 hours during the peak viral shedding of the infected hamsters in the central cage. At the completion of the air sterilization, the hamsters in the peripheral cages were immediately moved to a clean hamster cage and maintained for three days to evaluate if the hamsters became infected. The Infected hamsters were removed from the central cage and terminated. All hamsters were humanely euthanized and necropsied at the completion of the study.
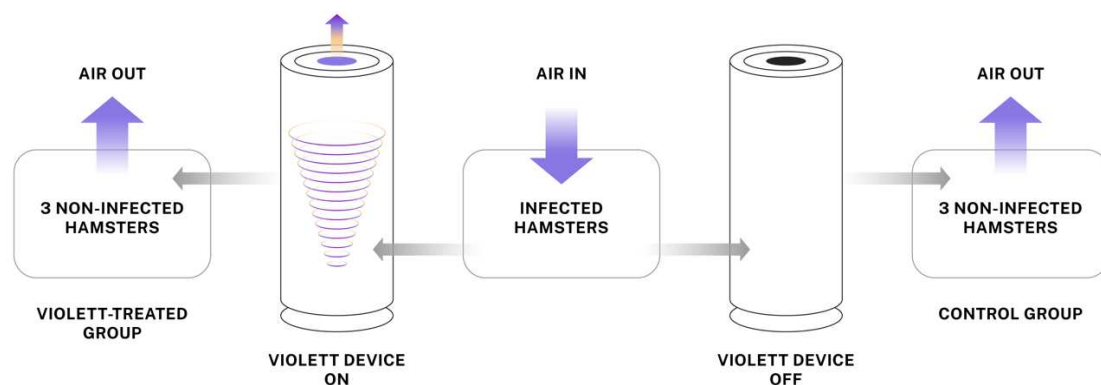
**Figure 1. Experimental airborne transmission of SARS-CoV-2 using a hamster model.** Hamsters were intranasally challenged with SARS-CoV-2 and transferred to center cage after 24 hours. Violett devices were placed in between infected hamster cage and non-infected hamster cages to treat air moving from the infected hamster cage into the periphery cages. The non-infected hamsters were exposed for 48 hours.

### Virus

SARS-CoV-2 propagation occurred in a BSL-3 laboratory setting. Virus (isolate USA-WA1/2020) was acquired through BEI Resources (product NR-52281) and amplified in Vero C1008 (Vero E6) cell culture. Vero E6 cells (ATCC CRL-1568) were cultured in Dulbecco's modified Eagle's medium (DMEM) supplemented with glucose, L-glutamine, sodium pyruvate, 5% fetal bovine serum (FBS) and antibiotics. Inoculation of Vero E6 cells with SARS-CoV-2 was carried out directly in DMEM containing 1% FBS.  Supernatant harvested from infected cells 3-4 days after inoculation was clarified by centrifugation at 800 x g, supplemented with FBS to 10% and frozen to -80°C in aliquots. The virus titer was determined using a standard double overlay plaque assay [13].

### Viral challenge

SARS-CoV-2 virus was diluted in phosphate buffered saline (PBS) to $1 \times 10^4$ pfu/0.1mL.   The hamsters were first lightly anesthetized with 10 mg of ketamine hydrochloride and 1 mg of xylazine hydrochloride. Each hamster was administered virus via pipette into the nares (50 µL/nare) for a total volume of 100 µL per hamster. Virus back-titration was performed on Vero E6 cells immediately following inoculation. Hamsters were observed until fully recovered from anesthesia.

### Oropharyngeal swabs

Oropharyngeal swabbing was performed on all hamsters prior to live virus challenge then daily after viral challenge to evaluate viral shedding. The swabbing was performed by inserting a sterile cotton swab and rotating the swab in the oropharyngeal area of the mouth for about 5 seconds. Swabs were placed in viral transport media (DMEM containing 2% FBS) supplemented with antibiotics and antifungal then stored at -80°C until further analysis.

### Clinical Observations

Body weights were recorded prior to viral exposure and then daily after exposure. Weights were recorded in grams. Clinical evaluations were performed daily during the study and included recording temperament, ocular discharge, nasal discharge, coughing/sneezing, dyspnea, lethargy, anorexia, and moribund.

### Tissue Collection

Necropsies were performed at three or five days after live virus challenge to determine gross pathological changes in respiratory tissues. Tissues were collected for virus quantification and histopathology. For virus quantitation, portions of right cranial lung lobe, right caudal lung lobe, and nasal turbinate specimens from each hamster were weighed (100 mg per specimen) and homogenized in viral transport media with antibiotics then frozen to −80 °C until the time of analysis. The tissue homogenates were briefly centrifuged and virus titers in the supernatant were determined by plaque assay. For histopathology, portions of the left lobe, right middle lung lobe, and trachea were collected from each hamster. The tissues were placed in 10% neutral buffered formalin for seven days then paraffin embedded and stained with hematoxylin and eosin using routine methods for histological examination.

### Virus Titration

Plaque assays were used to quantify infectious virus in oropharyngeal swabs and tissues. Briefly, all samples were serially diluted 10-fold in DMEM+ 1% FBS supplemented with antibiotics. Confluent Vero E6 cell monolayers were grown in 6-well tissue culture plates. The growth media was removed from the cell monolayers and washed with PBS immediately prior to inoculation. Each well was inoculated with 0.1 mL of the appropriate diluted sample. The plates were rocked every 10-15 minutes for 45 minutes and then overlaid with 0.5% agarose in media with 7.5% bicarbonate and incubated for 1 day at 37°C, 5% $CO_2$. A second overlay with neutral red dye was added at 24 hours and plaques were counted at 48-72 hours post-plating. Viral titers are reported as the $\log_{10}$ pfu per swab or gram (g). Samples were considered negative for infectious virus if viral titers were below the limit of detection (LOD). The theoretical limit of detection was calculated using the following equation:

$$LOD = \log [1/ (N \times V)]$$

where N is the number of replicates per sample at the lowest dilution tested; V is the volume used for viral enumeration (volume inoculated/well in mL). For oropharyngeal swabs the LOD was 10 pfu/swab or 1.0 $\log_{10}$ pfu/swab. For tissues the LOD was 100 pfu/g or 2.0 $\log_{10}$ pfu/g.

**Histopathology**

Histopathology was blindly interpreted by a board-certified veterinary pathologist. The H&E slides were evaluated for morphological evidence of inflammatory-mediated pathology in lung, and trachea, and reduction or absence of pathological features used as an indicator of protection against airborne SARS-CoV-2 exposure. Each hamster was assigned a score of 0-3 based on absent, mild, moderate, or severe manifestation, respectively, for each manifestation of pulmonary pathology including mural bronchial inflammation, neutrophilic bronchitis, consolidating pneumonia, and interstitial alveolar thickening, then the sum of all scores provided for each hamster. H&E-stained lung tissue slides were scanned at 20Å~ magnification using an Olympus VS120 microscope, Hamamatsu ORCA-R2 camera, and Olympus VS-ASW 2.9 software through the Experimental Pathology Facility at Colorado State University.

**Statistical analysis**

Group mean (n=3) viral titers of swabs and tissues were analyzed using a two-way ANOVA analysis followed by a post hoc test to analyze differences between groups. In the case where samples reached the LOD, values were entered as 0 for statistical analysis. Data were considered significant if $p < 0.05$. Composite pathology scores (n=3) were compared between groups using a one-way ANOVA analysis followed by a post hoc test to analyze difference between groups. Analysis was performed using GraphPad Prism software (version 9.2.0) (GraphPad Software, Inc, La Joia, CA).

## 3. Results

*Clinical Parameters*

Following viral exposure none of the hamsters in any of the groups displayed signs of disease and were clinically normal. From the time of viral exposure to necropsy, the Infected group on average lost about 4.8% body weight over the 3-day period. Conversely, the Violett treated group and the Control group gained body weight (average of 10.8% and 7.8%, respectively) over the course of 5 days (Figure 2). There was no statistical difference between the groups.

**Figure 2. Body weight changes in hamsters after live virus exposure**
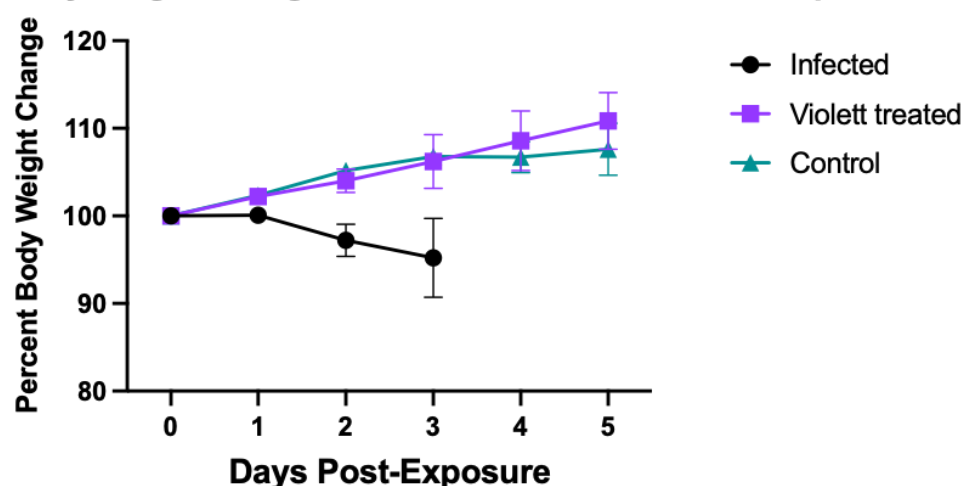
Body weight changes in hamsters as a percentage after viral exposure. Body weights were monitored daily for 3 days in the Infected group (n=9) and 5 days in the Control (n=9) and Violett (n=9) treatment groups. Data represented as the group mean +/- SD of the starting body weight.

*Virus titration*

We next investigated viral shedding in the oropharyngeal cavity in all hamsters. Hamsters were swabbed prior to viral exposure and then daily till day 3 for the Infected group and day 4 for the Violett treated and Control group. After intranasal challenge all hamsters in the Infected group had detectable infectious virus over the course of 3 days (except for one hamster on day 3)(Figure 3). Peak viral shedding was detected on 1 day post-infection (DPI) with a mean titer of 3.66 $\log_{10}$ pfu/ swab followed by a decline with a mean titer of 3.02 $\log_{10}$ pfu/ swab at 2 DPI and 1.92 $\log_{10}$ pfu/ swab at 3 DPI. Conversely, in the Control group, infectious virus was not detected in the swabs until 2 days post exposure to the Infected hamster group. The virus load increased to 2.65 $\log_{10}$ pfu/swab by day 4 indicating airborne transmission did occur to the Control group. The variability detected in the swabs over the course of the infection can be attributed to the lower challenge dose and the gradual progression of disease from the airborne exposure as compared to the Infected group. Of most interest, is the lack of detection of infectious virus in the oral cavity at any time point from the Violett treated group. The difference in viral titers between the Violett treated group and the Control group was statistically significant on day 3 (*p*=0.0013) and day 4 post-exposure (*p*<0.0001).

## Figure 3. Viral shedding from oropharyngeal swabs
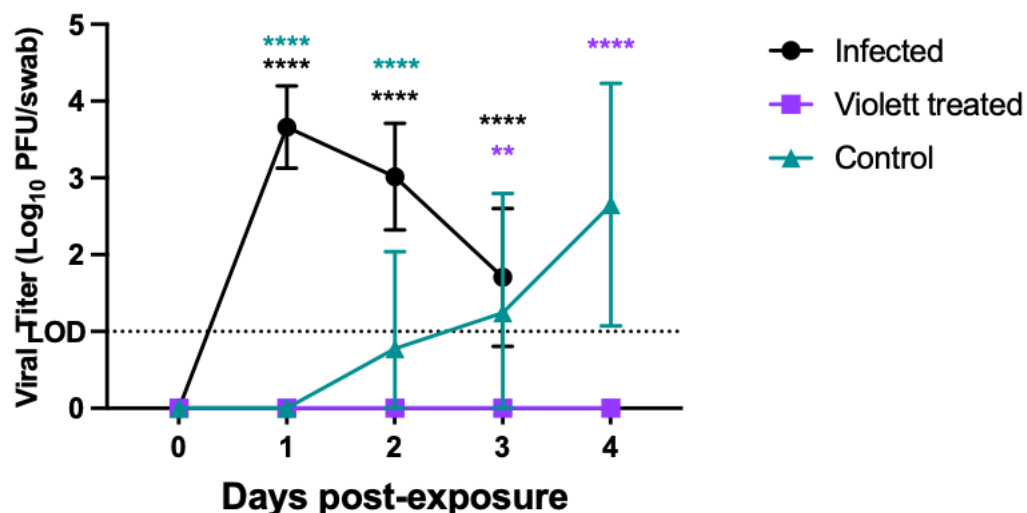
Viral loads in the oral pharyngeal swabs of hamster exposed to SARS-CoV-2. Viral titers were determined by plaque assay. Data points represent group mean +/- SD. LOD=Limit of detection denoted by horizontal dotted line. Asterisks in purple *** above bars indicate stastically significant difference in viral titers between the Violett treated and the Control groups (****p<0.0001, ** p<0.01). Asterisks in black *** above bars indicate stastically significant difference in viral titers between the Violett treated and the Infected groups (****p<0.0001). Asterisks in teal *** above bars indicate stastically significant difference in viral titers between the Control and the Infected groups (****p<0.0001).

To confirm protection from airborne transmission in the Violett treated group, upper and lower respiratory tract tissues were tested for viral replication. Nasal turbinate and lung tissues from the Infected group were collected 3 days after intranasal exposure with SARS-CoV-2 while tissues from the Control and Violett treated groups were collected 5 days after exposure. Previous experimental infections with SARS-CoV-2 Wuhan strain in a hamster model show that viral replication between the cranial and caudal lung lobes are similar [14]. However, the cranial lobe is usually affected first during a viral infection while the caudal lobe can become affected later in disease course [15]. Therefore both lobes were tested for viral replication. In the Infected group the viral titers in the turbinates had a mean of 6.21 $\log_{10}$ pfu/0.1g (Figure 4). The viral replication was slightly less in the lungs with a mean of 5.75 $\log_{10}$ pfu/ 0.1g in the cranial lungs and 6.03 $\log_{10}$ pfu/ 0.1g in the caudal

lungs. In the Control group, the viral titer mean was 5.99 $\log_{10}$ pfu/ 0.1g in the turbinates, 5.24 $\log_{10}$ pfu/ 0.1g in the cranial lungs, and 5.17 $\log_{10}$ pfu/ 0.1g in the caudal lungs. The titers were less than the infected group as expected and more representative of natural infections. In contrast, no infectious virus was detected in respiratory tissues in the Violett treated group demonstrating that the Violett device prevents airborne transmission of SARS-CoV-2 to naïve hamsters.

## Figure 4. Viral burden of respiratory tract tissues
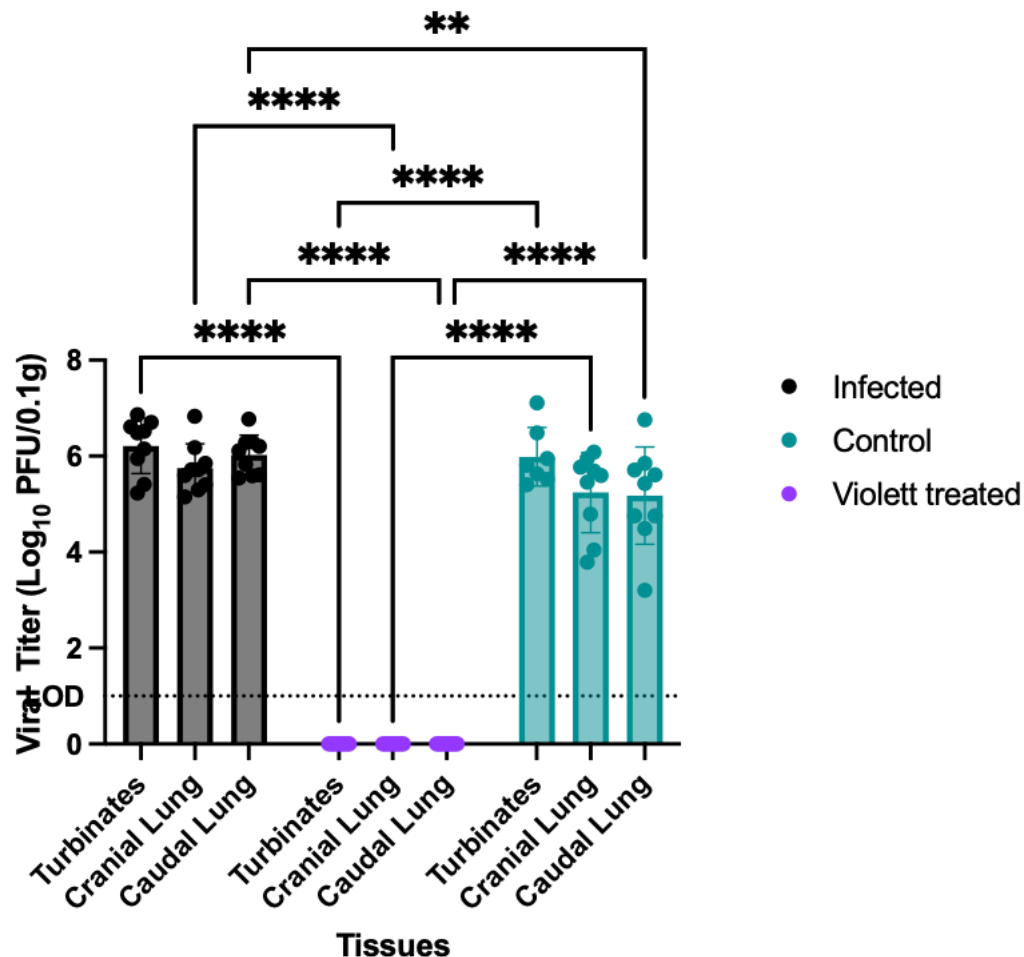
Viral replication in lower respiratory tract of hamster exposed to SARS-CoV-2. The presence of infectious virus was determined in turbinates, cranial lung lobe and caudal lung lobe of each hamster. Viral titers were determined by plaque assay. Data points represent group mean +/- SD. LOD=Limit of detection denoted by horizontal dotted line. Asterisks above bars indicate stastically significant difference in viral titers (****p<0.0001, ** p<0.01).

*Histopathology*

Hematoxylin and eosin (H&E) stained slides that included sections of lung and trachea, were reviewed for histopathological changes resulting from SARS-CoV-2 exposure (Figure 5).   Hamsters intranasally challenged with SARS-CoV-2 (Infected group) demonstrated the most severe pulmonary pathology. Histopathological features of SARS-CoV-2 infection in this group included bronchial hyperplasia of secondary and tertiary bronchi that ranged from segmental cellular piling to diffuse epithelial thickening. Alveolar septa were thickened by mononuclear inflammatory cell infiltrates and centered in regions of pneumonia or diffusely throughout all septa. Inflammation was appreciated in the trachea. The Control group has the largest degree of variability in overt lesion

burden but generally exhibited mild pathology compared to the infected group. Bronchi infiltrative inflammation, consolidated interstitial pneumonia, and thickening of alveolar walls was observed in most hamsters within the group. Similar to the Infected group, there was appreciable inflammation within the trachea in several hamsters. Minimal to no lesions were appreciated in the Violett treated group. Mild alveolar septa thickening was observed in some of the hamsters. However, the scoring was low and could be interpreted as within normal histological limits.

Based on pathology scoring of lung tissues, the Violett treatment effectively prevented SARS-CoV-2 replication and pathology in respiratory tissues. The Infected group had a mean composite score of 7.2, the Control group had a mean composite score of 3.7, while the Violett-treated group had a significantly lower mean composite score of 0.28 (Figure 6). The difference in composite score were statistically significant between the Violett treated and the Infected group ( $p<0.0001$) and the Violett treated group and the Control group ($p$=0.0004). All hamsters in the Infected group had appreciable lung lesions demonstrating the robustness of viral replication from intranasal challenge. The degree of lesions observed in the Control group was more variable compared to the Infected group, however, it is evident that airborne transmission from the Infected to the Control group did occur. The Violett treatment prevented the development of COVID disease in the lungs of naïve hamsters.
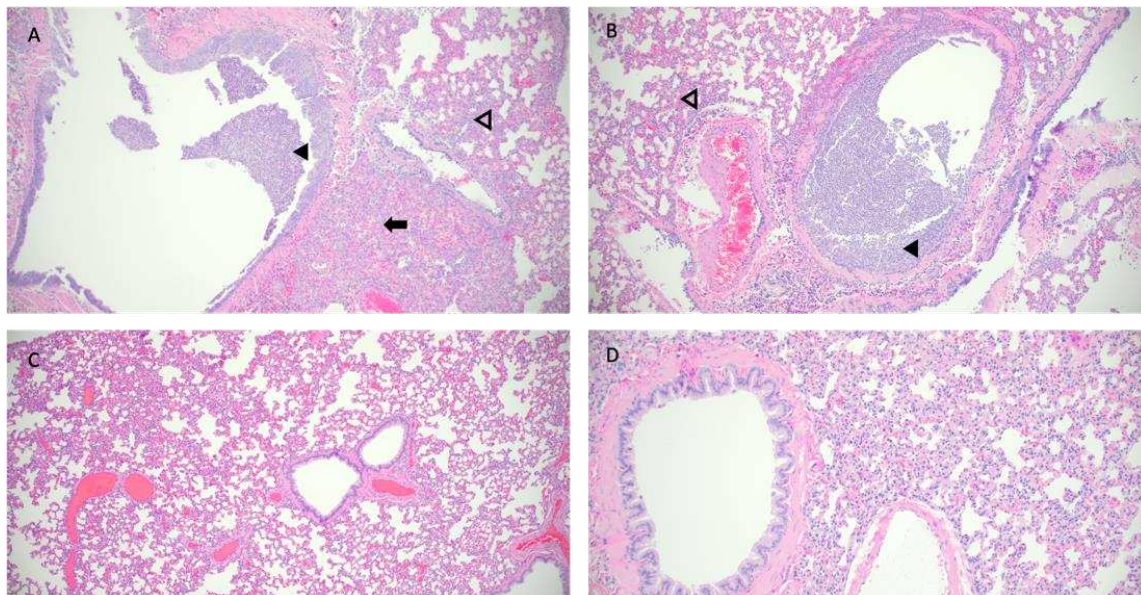
**Figure 5. Pathological findings in hamster lungs**. Representative histology of differences between intranasally infected (A), non-treated control (B), Violett-treated (C ), and uninfected control (D). Image A is taken at 3 days post challenge and images B and C are taken at   5 days post exposure. Infected hamsters (A,B) show consolidating interstitial pneumonia (arrow), thickening of alveolar walls (open arrowhead), and accumulation of neutrophils within bronchus lumen (solid arrowhead). Minimal evidence of interstitial pneumonia and an absence of epithelial regeneration in the Violett-treated hamsters (C ). Images taken at 10x magnification.

## Figure 6. Composite histopathology score
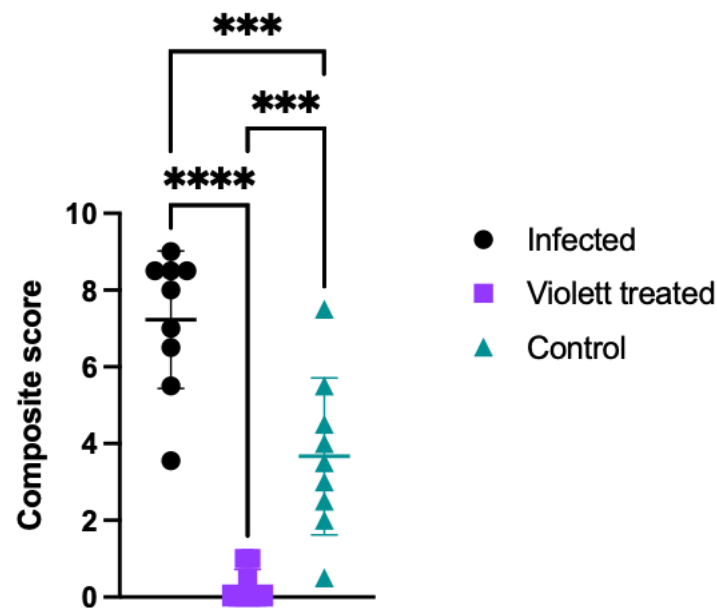
Two sections of lung per hamster were evaluated. Sections were evaluated separately and then averaged to provide a mean score for that animal. Means of each parameter were added to provide a composite score. Data points represent mean +/- SD. Astricks above bars indicate statistically significant difference in composite score (****p<0.0001, ***p<0.001).

## 4. Discussion

UV-C inactivation has gained widespread recognition for its efficacy against various pathogens, including viruses and bacteria [16]. With the rapid spread of SARS-CoV-2, environmental and structural changes became a valuable tool to reducing transmission in areas with high risk of exposure [17]. As we move out of a pandemic state, we continue to face uncertainty with newly emerging variants. These variants contain mutations that can enhance antibody evasion and increase transmissibility [18,19]. A multi-prong approach is needed to provide protective immunity and reduce exposure risk. Notably, environmental measures such as UV light treatment will be critical in mitigating viral transmission.

UV-C light has been successfully applied to inactivate SARS-CoV-2 in air [11,20]. The fundamental mechanism of UV-C light relies on destroying the bonds within the DNA of viruses and bacteria, and as that is the fundamental building block of all life on Earth it can be considered pathogen agnostic. While this study focused on transmission of SARS-CoV-2, this can be seen as a readout for any number of airborne diseases both known and still to be identified. The development of this kind of technology allows us to future proof our healthcare systems for the rise of new variants or even new diseases.

Previous studies have corroborated the efficacy of UV-C light in preventing airborne SARS-CoV-2 transmission in a hamster model. Hamsters are a well-established animal model for SARS-CoV-2 airborne transmission studies [21–24]. Bowen et al. demonstrated protection from airborne transmission with the use of a UV-C device over a 48 hour period of exposure [9]. Individual hamsters housed in UV-C air treated caging did not have viral replication at three days after exposure. To evaluate efficacy against VOCs, Fischer et al. tested both the WA-1 and the Delta strain against a UV-C device [8]. In the study two, naïve hamsters were exposed via aerosols from infected hamsters for a total of four hours then orally swabbed for three days and maintained till 14 days post exposure to determine if transmission occurred. All treated hamsters were protected from airborne transmission

of both the WA-1 and Delta strains. The present work further confirms the effectiveness of UV-C in preventing airborne transmission of SARS-CoV-2. We demonstrate the robustness of Violett device to prevent transmission during peak viral shedding in a group setting of susceptible hosts.

The length of exposure in these studies is of particular note. This more accurately mimics a shared room in a medical setting (ex. Hospital) and indicates a level of protection that would be meaningful to a real world setting with elevated risk from prolonged exposure. The risk of prolonged exposure extends beyond the medical setting as well. The Violett device would provide added safety to children in schools, patients in waiting rooms, and workers in offices. The portable nature of the Violett device means that it can be flexibly used in a variety of settings where large numbers of people gather for extended periods of time.

There is nothing more fundamental to our health and well-being than the air we breathe. The global pandemic has shown how devasting airborne diseases can be to both healthy individuals and especially to our most vulnerable populations. Beyond the risk of disease and associated morbidity, the social and emotional toll of isolation over the last few years has been extreme. The spike in mental health issues and depression that's being seen as a direct result of this pandemic is just beginning to be documented but the numbers are alarming. The picture is even more severe when you look at higher risk groups such as older adults or immune compromised patients. This isolation leads to lower compliance with medication and health directives which can cause severe medical complications [25]. The Violett UV-C sterilization device offers a solution to create safer environments for both healthcare workers and patients, presenting a crucial step toward mitigating health threats caused by airborne pathogens.

## 5. Patents

USPTO application number for the Violett technology is 17574159.

**Author Contributions**: Conceptualization, I.R., J.P., W.D., L.H., B.D.; Methodology, I.R., W.D.; Data Curation, I.R., L.H.; Original Draft Preparation, I.R., L.H., J.P, W.D., B.D.; Review & Editing, I.R., J.P., B.D.; Visualization, I.R., L.H., J.P.; Funding Acquisition, I.R., J.P., B.D.

**Funding:** Funding provided by internal funds from Colorado State University. Violett Inc provided material support.

**Data Availability Statement:** Not applicable.

**Acknowledgments:** The histologic preparation, pathologic interpretation and photomicrographic work was performed by the Experimental Pathology facility at Colorado State University, RRID:SCR_23562. The following reagent was deposited by the Centers for Disease Control and Prevention and obtained through BEI Resources, NIAID, NIH: SARS-Related Coronavirus 2, Isolate hCoV-19/USA-WA1/2020, NR-52281.

**Conflicts of Interest:** Authors Perez, Davenport, and Doyle were employees of Violett at the time of the study and were involved in construction of device and manuscript review. All data and analyses were collected and performed without input from Violett.

## References

1. World Health Organization WHO Coronavirus (COVID-19) Dashboard 2020. Available online at: https://covid19.who.int (Accessed 02 September 2023).
2. Li, H.; Wang, Y.; Ji, M.; Pei, F.; Zhao, Q.; Zhou, Y.; Hong, Y.; Han, S.; Wang, J.; Wang, Q.; et al. Transmission Routes Analysis of SARS-CoV-2: A Systematic Review and Case Report. *Front. Cell Dev. Biol.* **2020**, *8*, 618, doi:10.3389/fcell.2020.00618.
3. Ahlawat, A.; Mishra, S.K.; Birks, J.W.; Costabile, F.; Wiedensohler, A. Preventing Airborne Transmission of SARS-CoV-2 in Hospitals and Nursing Homes. *Int. J. Environ. Res. Public. Health* **2020**, *17*, 8553, doi:10.3390/ijerph17228553.
4. Addleman, S.; Leung, V.; Asadi, L.; Sharkawy, A.; McDonald, J. Mitigating Airborne Transmission of SARS-CoV-2. *CMAJ Can. Med. Assoc. J. J. Assoc. Medicale Can.* **2021**, *193*, E1010–E1011, doi:10.1503/cmaj.210830.
5. Bundgaard, H.; Bundgaard, J.S.; Raaschou-Pedersen, D.E.T.; von Buchwald, C.; Todsen, T.; Norsk, J.B.; Pries-Heje, M.M.; Vissing, C.R.; Nielsen, P.B.; Winsløw, U.C.; et al. Effectiveness of Adding a Mask

Recommendation to Other Public Health Measures to Prevent SARS-CoV-2 Infection in Danish Mask Wearers : A Randomized Controlled Trial. *Ann. Intern. Med.* **2021**, *174*, 335–343, doi:10.7326/M20-6817.

6.  van der Valk, J.P.M.; In 't Veen, J.C.C.M. SARS-Cov-2: The Relevance and Prevention of Aerosol Transmission. *J. Occup. Environ. Med.* **2021**, *63*, e395–e401, doi:10.1097/JOM.0000000000002193.

7.  Shah, A.S.V.; Gribben, C.; Bishop, J.; Hanlon, P.; Caldwell, D.; Wood, R.; Reid, M.; McMenamin, J.; Goldberg, D.; Stockton, D.; et al. Effect of Vaccination on Transmission of SARS-CoV-2. *N. Engl. J. Med.* **2021**, *385*, 1718–1720, doi:10.1056/NEJMc2106757.

8.  Fischer, R.J.; Port, J.R.; Holbrook, M.G.; Yinda, K.C.; Creusen, M.; Ter Stege, J.; de Samber, M.; Munster, V.J. UV-C Light Completely Blocks Aerosol Transmission of Highly Contagious SARS-CoV-2 Variants WA1 and Delta in Hamsters. *Environ. Sci. Technol.* **2022**, *56*, 12424–12430, doi:10.1021/acs.est.2c02822.

9.  Bowen, R.A.; Gilgunn, P.; Hartwig, A.E.; Mullen, J. Prevention of Airborne Transmission of SARS-CoV-2 by UV-C Illumination of Airflow. *COVID* **2021**, *1*, 602–607, doi:10.3390/covid1030050.

10. Jureka, A.S.; Williams, C.G.; Basler, C.F. Pulsed Broad-Spectrum UV Light Effectively Inactivates SARS-CoV-2 on Multiple Surfaces and N95 Material. *Viruses* **2021**, *13*, 460, doi:10.3390/v13030460.

11. Biasin, M.; Bianco, A.; Pareschi, G.; Cavalleri, A.; Cavatorta, C.; Fenizia, C.; Galli, P.; Lessio, L.; Lualdi, M.; Tombetti, E.; et al. UV-C Irradiation Is Highly Effective in Inactivating SARS-CoV-2 Replication. *Sci. Rep.* **2021**, *11*, 6260, doi:10.1038/s41598-021-85425-w.

12. Inagaki, H.; Saito, A.; Sugiyama, H.; Okabayashi, T.; Fujimoto, S. Rapid Inactivation of SARS-CoV-2 with Deep-UV LED Irradiation. *Emerg. Microbes Infect.* **2020**, *9*, 1744–1747, doi:10.1080/22221751.2020.1796529.

13. Baer, A.; Kehn-Hall, K. Viral Concentration Determination Through Plaque Assays: Using Traditional and Novel Overlay Systems. *J. Vis. Exp.* **2014**, 52065, doi:10.3791/52065.

14. Imai, M.; Iwatsuki-Horimoto, K.; Hatta, M.; Loeber, S.; Halfmann, P.J.; Nakajima, N.; Watanabe, T.; Ujie, M.; Takahashi, K.; Ito, M.; et al. Syrian Hamsters as a Small Animal Model for SARS-CoV-2 Infection and Countermeasure Development. *Proc. Natl. Acad. Sci.* **2020**, *117*, 16587–16595, doi:10.1073/pnas.2009799117.

15. Francis, M.E.; Goncin, U.; Kroeker, A.; Swan, C.; Ralph, R.; Lu, Y.; Etzioni, A.L.; Falzarano, D.; Gerdts, V.; Machtaler, S.; et al. SARS-CoV-2 Infection in the Syrian Hamster Model Causes Inflammation as Well as Type I Interferon Dysregulation in Both Respiratory and Non-Respiratory Tissues Including the Heart and Kidney. *PLoS Pathog.* **2021**, *17*, e1009705, doi:10.1371/journal.ppat.1009705.

16. Reed, N.G. The History of Ultraviolet Germicidal Irradiation for Air Disinfection. *Public Health Rep. Wash. DC 1974* **2010**, *125*, 15–27, doi:10.1177/003335491012500105.

17. Dowell, D.; Lindsley, W.G.; Brooks, J.T. Reducing SARS-CoV-2 in Shared Indoor Air. *JAMA* **2022**, *328*, 141–142, doi:10.1001/jama.2022.9970.

18. Carabelli, A.M.; Peacock, T.P.; Thorne, L.G.; Harvey, W.T.; Hughes, J.; COVID-19 Genomics UK Consortium; de Silva, T.I.; Peacock, S.J.; Barclay, W.S.; de Silva, T.I.; et al. SARS-CoV-2 Variant Biology: Immune Escape, Transmission and Fitness. *Nat. Rev. Microbiol.* **2023**, doi:10.1038/s41579-022-00841-7.

19. Sun, C.; Xie, C.; Bu, G.-L.; Zhong, L.-Y.; Zeng, M.-S. Molecular Characteristics, Immune Evasion, and Impact of SARS-CoV-2 Variants. *Signal Transduct. Target. Ther.* **2022**, *7*, 202, doi:10.1038/s41392-022-01039-2.

20. Raeiszadeh, M.; Adeli, B. A Critical Review on Ultraviolet Disinfection Systems against COVID-19 Outbreak: Applicability, Validation, and Safety Considerations. *ACS Photonics* **2020**, *7*, 2941–2951, doi:10.1021/acsphotonics.0c01245.

21. Sia, S.F.; Yan, L.-M.; Chin, A.W.H.; Fung, K.; Choy, K.-T.; Wong, A.Y.L.; Kaewpreedee, P.; Perera, R.A.P.M.; Poon, L.L.M.; Nicholls, J.M.; et al. Pathogenesis and Transmission of SARS-CoV-2 in Golden Hamsters. *Nature* **2020**, *583*, 834–838, doi:10.1038/s41586-020-2342-5.

22. Zhang, X.; Chen, S.; Cao, Z.; Yao, Y.; Yu, J.; Zhou, J.; Gao, G.; He, P.; Dong, Z.; Zhong, J.; et al. Increased Pathogenicity and Aerosol Transmission for One SARS-CoV-2 B.1.617.2 Delta Variant over the Wild-Type Strain in Hamsters. *Virol. Sin.* **2022**, *37*, 796–803, doi:10.1016/j.virs.2022.09.008.

23. Boon, A.C.M.; Darling, T.L.; Halfmann, P.J.; Franks, J.; Webby, R.J.; Barouch, D.H.; Port, J.R.; Munster, V.J.; Diamond, M.S.; Kawaoka, Y. Reduced Airborne Transmission of SARS-CoV-2 BA.1 Omicron Virus in Syrian Hamsters. *PLoS Pathog.* **2022**, *18*, e1010970, doi:10.1371/journal.ppat.1010970.

24. Port, J.R.; Yinda, C.K.; Owusu, I.O.; Holbrook, M.; Fischer, R.; Bushmaker, T.; Avanzato, V.A.; Schulz, J.E.; Martens, C.; van Doremalen, N.; et al. SARS-CoV-2 Disease Severity and Transmission Efficiency Is Increased for Airborne Compared to Fomite Exposure in Syrian Hamsters. *Nat. Commun.* **2021**, *12*, 4985, doi:10.1038/s41467-021-25156-8.

25. National Academies of Sciences, Engineering, and Medicine; Division of Behavioral and Social Sciences and Education; Health and Medicine Division; Board on Behavioral, Cognitive and Sensory Sciences; Board of Health Sciences Policy; Committee on the Health and Medical Dimensions of Social Isolation and Loneliness in Older Adults Health Impacts of Social Isolation and Loneliness on Morbidity and Quality of Life. In *Social Isolation and Loneliness in Older Adults: Opportunities for the Health Care System*; National Academies Press (US): Washington (DC), 2020; p. Chapter 3.